applied sciences

MDPI

Article

Assessment of the Long-Term Leaching Behavior of Incineration Bottom Ash: A Study of Two Waste Incinerators in Germany

Franz-Georg Simon * and Philipp Scholz

BAM Bundesanstalt für Materialforschung und-prüfung, 12205 Berlin, Germany; philipp.scholz@bam.de
* Correspondence: franz-georg.simon@bam.de

Abstract: The long-term leaching behavior of incineration bottom ash (IBA) was studied with large-scale samples from two German waste incinerators with grate technology. The observation period was up to 281 days. The aging processes proceeded faster in the outdoor storage of the samples. The dominant factor in the leaching behavior is the pH, which starts at values above 12 and decreases to values below 10 (outdoors, <11 indoors). Most heavy metals exhibit minimum solubility in this pH range. The solubility of Sb depends on the prevailing Ca concentration, due to the formation of low-soluble Ca antimonate. The very low sulfate concentrations observed in the leaching tests with fresh IBA could be explained by the presence of ettringite. In the course of the aging reaction, ettringite is transformed into gypsum. The results from batch tests were compared with those from column tests, showing reasonable agreement. Leaching dynamics can be better followed with column tests. All results confirm that the use of IBA is possible under German law.

Keywords: aging; incineration bottom ash; leaching; secondary building materials

Citation: Simon, F.-G.; Scholz, P. Assessment of the Long-Term Leaching Behavior of Incineration Bottom Ash: A Study of Two Waste Incinerators in Germany. *Appl. Sci.* **2023**, *13*, 13228. https://doi.org/10.3390/app132413228

Academic Editors: Rafael López Núñez and Apostolos Giannis

Received: 15 November 2023
Revised: 6 December 2023
Accepted: 11 December 2023
Published: 13 December 2023

1. Introduction

The global generation of municipal solid waste (MSW) was 2.1 billion tons per year (reported data collected from 2011–2017) and is expected to increase to 3.4 billion tons by 2050 [1]. The report assumes that at least 33% of this amount is simply dumped, without complying with environmental standards. According to the available data on the country level, 13.1% is incinerated, i.e., 272 million tons, enabling a high degree of hygienization for the treated waste. Furthermore, waste incineration results in a 90% reduction of waste volume. However, solid residues such as bottom ash and products from air pollution control (APC), i.e., fly ash, residues from dry or semi-dry APC systems, or sludge from waste water treatment are produced [2]. Incineration bottom ash (IBA) constitutes the largest residual fraction at approximately 25%, while APC residues vary between 2–5%, depending on the specific APC system [3].

IBA from waste incineration consists of solid phases such as glass, ceramics, ash, and metals (ferrous, Fe; and non-ferrous, NFe) already contained in the MSW, as well as new phases that are formed during the incineration process [4–7]. The recovery of elemental metals from IBA is nowadays state-of-the-art technology for ferrous and also non-ferrous metals [8]. High revenues are achieved for the NFe metals, especially for copper and brass. The five main chemical elements in IBA are Si, Ca, Fe, Al, and Na. While Si and Ca are bound as oxides and silicates, Al and Fe occur not only as oxides but also in their elemental form. Na is also present as chloride, Ca also as sulfate [3]. IBA is an extremely inhomogeneous material, and its exact composition depends greatly on the type of waste incinerated, the conditions of incineration, and further treatment steps [4,9,10]. A typical IBA composition [4,11,12] is as follows:

- 9% inert material (glass, ceramics, stones, etc.);
- 1% unburned (residual organic matter);
- 10% metals (8% Fe metals and 2% NFe, mainly Al and Cu or Cu alloys);

- 40% ash;
- 40% melted products (slag).

The APC residues contain considerably more heavy metals and organic pollutants, such as dioxins and furans, which hampers use of the material [13]. Using IBA, usually after a treatment in which at least the elemental metals are separated, is widely accepted [14]. The treatment processes are described in detail elsewhere [8,15–19]. An important use pathway is as a sub-base material for road construction [20,21].

A three-month aging period has been established as the common practice for initial treatment of bottom ash before reuse applications. In the course of this aging, contaminants are immobilized by processes like carbonation, hydration, and oxidation. In particular, the leaching of heavy metals is reduced to environmentally acceptable levels as required for disposal of IBA on landfills [22]. The leaching behavior of ashes is influenced by parameters such as the pH of the leaching solution, the redox potential (pE), the liquid-to-solid ratio (L/S in L/kg), and the contact time or flow velocity (in column percolation tests) [23–25]. For most heavy metals, the pH value during the leaching test is the dominant factor. In contact with water, IBA reacts alkaline due to the presence of $Ca(OH)_2$, a reaction product from CaO formed during the incineration process. From the solubility product of $Ca(OH)_2$ ($K_L = 5.5 \times 10^{-6}$ mol^3 L^{-3} [26]), a maximum pH of 12.35 can be calculated. Observed pH values in standard leaching tests are even higher. During aging, calcium oxide and hydroxide in IBA react with CO_2 from the atmosphere (or rain in the case of outdoor storage) and forms $CaCO_3$, which is almost insoluble, and therefore does not react alkaline. The observed pH values in the leaching test decrease, and so does the concentration of most heavy metals. The leaching of chloride and sulfate is less influenced by the pH [27], but is also relevant for use. The legal requirements for using IBA in Europe have recently been reviewed by an expert group [14]. The set limit values address the release of contaminants during use (mainly heavy metals and salts), emphasizing the importance of the leaching behavior. It has been stated that the overall utilization rate of IBA is approximately 54%. An upcoming issue is the classification of IBA according to the European List of Waste (LoW). The assessment of the ecotoxicity (hazardous property HP 14) of IBA is still under discussion [28,29]. Requirements for the total content of constituents are rarely defined for landfilling or using IBA; instead, leaching limit values are set. Therefore, the leaching behavior of IBA has been the topic of various research and review articles [30–36].

The present study was performed with three main objectives: (1) to investigate the leaching behavior of IBA in the course of the aging process for up to 281 days through batch tests with constant L/S ratios and column leaching tests, allowing a comparison of the different leaching approaches; (2) to compare the leaching data obtained with modelling results using the geochemical software Visual MINTEQ 3.1 [37], based on MinteqA2 [38], to identify relevant species in the leaching processes and to enable the prediction of heavy metal concentrations in the leachates; and (3) to perform nearly complete chemical analyses of leachates and solid contents, making it possible to elucidate the reaction mechanisms in the aging process. Finally, conclusions are drawn on the use of IBA as secondary building material.

2. Materials and Methods

Bottom ash samples from two different waste incineration plants in Germany (plant A and plant B, both using grate technology with a wet extraction system) were taken right after leaving the wet extraction unit of the incinerator and the subsequent removal of ferrous and non-ferrous metals through magnet and eddy current separation (sample A: 15 June 2021, sample B: 22 March 2023). Sample size was in the range of 400–600 kg each, large enough to generate homogenous test samples for the investigations performed in the lab. Batch tests were performed according to DIN 19529 [39] (L/S = 2 L/kg) and DIN EN 12457 [40] (L/S 10 L/kg). A representative sample mass of approximately 2.5 kg for each test was split into several subsamples, which were shaken in several glass bottles for 24 h. After 15 min of settling, the supernatants were recombined. Pressure filtration was

subsequently conducted through a 0.45-µm cellulose nitrate membrane filter for liquid-solid separation. All leaching tests were performed at least twice. Column tests were performed according to DIN 19528 [41] up to an L/S ratio of 10 L/kg. According to the standard, an L/S ratio of only 4 L/kg is required for basic characterization (or even L/S = 2 L/kg for the compliance test option in Germany). In column tests, the eluate is generated continuously over the complete test duration. Concentrations can therefore be determined for individual L/S ratios. DIN 19528 prescribes the L/S ratios as 0.3, 1.0, 2.0, and 4.0 L/kg; in this study, we also examined L/S = 7 L/kg and 10 L/kg. For a comparison of results from batch and column tests at different L/S ratios, the respective concentrations in mg/L were converted to leached amount E in mg/kg by multiplying by the respective liquid-to-solid ratio (L/S in L/kg). For the batch tests, this ratio is commonly 2 or 10 L/kg.

To determine the total concentration of most elements as cations (Al, As, B, Ba, Ca, Co, Cd, Cr, Cu, Fe, Hg, K, Mg, Mn, Mo, Na, Ni, P, Pb, S, Sb, Se, Si, Sn, Sr, Ti, Tl, V, Zn), a digestion using aqua regia was performed according to DIN ISO 11466 [42]. For this purpose, 0.5 g of the ground sample was placed in a PTFE container, and 12 mL of aqua regia (HNO_3 65% 3:1 HCl 37%) was added. Subsequently, the container was subjected to microwave digestion using an Albert Romera ATC-400 microwave for 20 min. The cations were analyzed using a Thermo Scientific iCAP 7000 ICP-OES equipped with an ASX-200 autosampler. Prior to sample measurements, calibration using external standards was necessary. For lower cation concentrations, additional ICP-MS measurements were carried out using a Thermo Scientific iCAP Qc instrument with the same aqua regia digestions.

For anion determination (F^-, Cl^-, $NO_2{}^-$, Br^-, $NO_3{}^-$, $SO_4{}^{2-}$, $PO_4{}^{3-}$), extractions with Na_2CO_3 were performed. In this procedure, 1 g of the sample and 10 g of Na_2CO_3 were brought to a boil with 100 mL of water under agitation and maintained at this temperature for 10 min. Subsequently, hot filtration was conducted, and the final volume was adjusted to 250 mL. Ion chromatography was performed using a Thermo Scientific Dionex Integrion system equipped with a Dionex Suppressor ADRS 600, an AS-AP autosampler, and a KOH gradient to determine the concentration of anions.

IBA was leached in the acidic pH range with maleic acid at pH 4. Maleic acid was chosen as the acidifying agent as suggested in the practice note of the German associations ITAD and IGAM for the assessment of HP 14 properties [43] of IBA [44,45]. In brief, 1 g of sample (milled to <0.25 mm grain size) was used in a triple approach. An amount of 40 mL of an extraction solution, containing 0.1 mol/L maleic acid and 0.1 mol/L sodium acetate, was added to the samples in centrifuge tubes. To adjust the pH to 4.0, 1.5 mol/L nitric acid or 1.0 mol/L sodium hydroxide solution was slowly added. The tubes were then shaken at 150 rpm for 24 h. After 1, 2, 4, and 6 h, the pH was adjusted to 4.0 with the previously mentioned chemicals, if necessary. After 24 h, the tubes were centrifuged at 6000 rpm, the eluate was collected, and residues were twice washed with 4 mL of water and centrifuged again. Finally, the tubes were filled up to 50 mL with water, i.e., the L/S ratio was 50 L/kg. For cation analyses using ICP-OES and ICP-MS, the samples were additionally acidified with concentrated nitric acid.

Aging experiments were carried out with samples A and B, each lasting approximately 3 months. Polyethylene containers (78 × 49 × 32 cm) were used for this purpose, each filled with approximately 50 kg of fresh bottom ash, prepared 3–5 days after sampling in the waste incineration plants. These containers were subjected to outdoor weather conditions on a rooftop (samples A and B outdoor) and, for comparison, stored indoors in a facility (samples A and B, indoor). The experimental setup was fundamentally the same for both ash samples. However, variations in the aging experiments were expected due to differing levels of rainfall, thus causing some differences in the results. Over the period from 30 June 2021 to 29 September 2021, the weathered outdoor sample A experienced a total of 348 L/m^2 of precipitation, whereas sample B recorded only 87 L/m^2 of precipitation from 31 March 2022 to 27 June 2022. Initially, sampling occurred on a weekly basis, with the intervals between samplings being extended later as minimal changes were anticipated. The methodology is displayed in Figure 1.

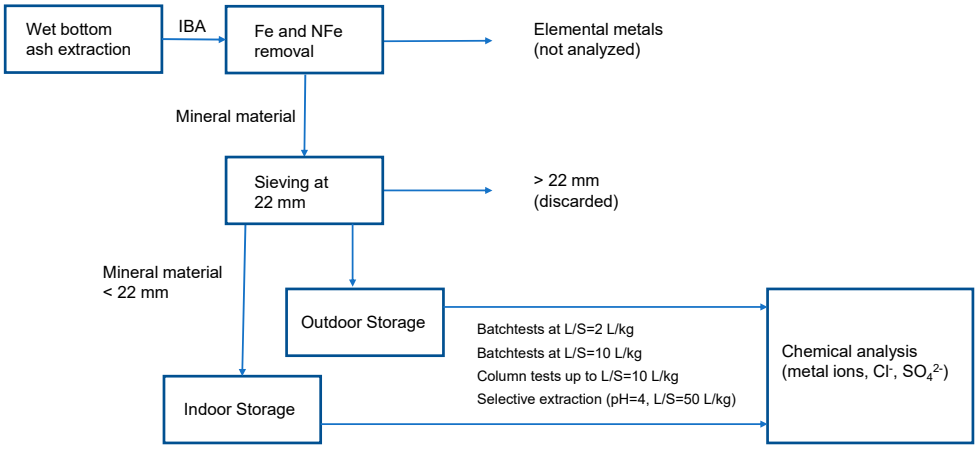

Figure 1. Flow chart of the methodology applied in the present study.

3. Results

Table 1 shows the total content of substances in the two bottom ash samples used for the aging experiment compared with data from the literature. The experiments were performed with the grain size fraction <22 mm; material >22 mm was excluded from the investigation. The mean values of triplicate analyses are presented for samples A and B. However, it is known that IBA is an extremely inhomogeneous material. For comparison, data from the literature (mean values, together with minimum and maximum values) are also shown in Table 1.

Table 1. Total content of substances in the test material in mg/kg (extraction with aq. regia, exception labelled). Ferrous and non-ferrous metals were removed from the IBA samples on site, at a technical scale.

Element	Sample A	Sample B	Literature [1] [46]
Ca	67,793	76,417	130,833 (50,825–198,289)
Si [2]	224,100	161,800	82,713 (6106–96,078)
Fe	38,530	52,932	58,714 (34,216–11,822)
Al	15,098	16,490	47,232 (30,527–75,089)
Na	10,916	9599	21,379 (12,308–34,791)
Mg	4781	4655	12,429 (6377–34,372)
K	3663	2504	7748 (4854–12,722)
P	3247	4378	5633 (2531–12,556)
Ti	2687	2661	4244 (2873–7479)
S	2853	3785	3862 (131–16,808)
Cu	1216	2883	3275 (738–17,620)
Zn	1671	2504	3241 (1142–9370)
Pb	475	418	1309 (197–6441)
Mn	546	929	1173 (644–2248)
Ba	774	1483	1102 (760–297)
Cr	28	180	353 (115–852)
Sr	132	213	271 (267–369)
B	89.5	26.1	198 (30–532)
Ni	85.0	100.8	185 (38–850)
Sn [2]	134.7	213.0	181 (52–737)
Sb	54.1	88.4	73 (18–250)
V	16.5	15.3	41.2 (19–248)
Co	35.7	32.9	31.8 (11–103)
Mo	4.4	8.2	30.1 (5–84)

Table 1. *Cont.*

Element	Sample A	Sample B	Literature [1] [46]
As	7.8	34.2	17.3 (4.4–73.2)
Cd	1.9	1.1	4.8 (1.1–117)
Carbonate (%) [3]	5.4	5.0	12,215 (5232–20,760)
LOI (%) [4]	1.93	1.8	1.0 (0.1–4.2)
Chloride [5]	2318	4485	9211 (3644–37,633)
Sulfate [5]	7337	16,544	11,586 (393–50,424)

[1] Data format: mean value (min-max); [2] analyzed by X-ray fluorescence analysis; [3] as $CaCO_3$, analyzed by gas volumetry; [4] analyzed gravimetrically after thermal treatment at 500 °C; [5] analyzed by ion chromatography (see anion determination in methodology section).

Standardized batch tests were performed at L/S ratios of 2 and 10 L/kg. The sample size for the batch tests were 500 and 100 g per liter, respectively. Effects of inhomogeneity are here less relevant than in the analysis of the total content using aqua regia with a sample size of 0.5 g. The presence of, e.g., a small metallic Cu or brass particle could lead to high Cu or Zn values after digestion even after careful lab sample preparation, whereas the impact in the leaching test would be small. The observed pH values of the leaching tests shortly after sampling ("fresh" IBA) were between 12.3 and 12.5, without any significant differences between the two L/S ratios. In the course of the aging experiment ("aged" IBA), the pH values dropped to values below 10 for the material stored outdoors and below 11 for the material stored indoors. Further, the decline in pH in the leaching tests was faster for the outdoor samples than for the samples stored indoor. The alkaline pH values are due to the presence of CaO and $Ca(OH)_2$ in IBA, which reacts with CO_2 from the air or in rain forming $CaCO_3$ [47]. As a result, pH values decrease to lower values. Figure 2 shows the pH curves (separated for indoors and outdoors) as a function of storage time. Obviously, the aging process is more efficient under outdoor conditions involving rainwater. The reason for that could be a more effective penetration of CO_2 containing rainwater through the material, compared to the heterogeneous gas-solid reaction only. The complete numerical data set can be found in the Supporting Information (SI), SI Table S1.

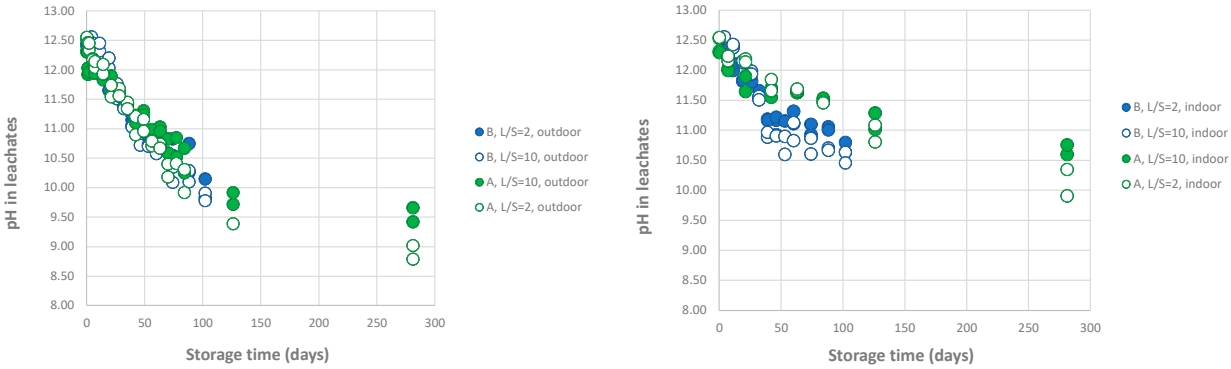

Figure 2. pH values measured at the end of the batch leaching test performed with samples A and B. Filled symbols are results at an L/S ratio of 10 L/kg, unfilled symbols at an L/S ratio of 2 L/kg. Green: sample A, blue: sample B. The decline of pH in the leaching test is faster for samples stored outside and goes to lower values (see text).

The leaching of most heavy metals is a function of pH. In the present investigation, the release of heavy metals was observed at the pH values at the end of the standardized batch test, ranging between 12.5 and 8.8 (sample A after 281 days; see Figure 2), and at a pH of 4 (leaching with maleic acid). In order to compare the experimental results obtained at different L/S ratios and during leaching with maleic acid, the concentrations were converted to leached amount (E) in mg/kg. A significant dependence of the release as

a function of pH was observed for Cu, Zn, Pb, and Sb, as displayed in Figure 3. Differences in the leached amount at the two different L/S ratios, as well as between outdoor and indoor storage, were not significant. Cu, Zn, and Pb showed a parabolic curve with minimum release in the range of pH 9–10. The reason for this behavior in the alkaline branch of the curve is the formation of soluble hydroxo complexes with the formulas $Me(OH)_3^-$ and $Me(OH)_4^{2-}$ at high pH values, i.e., high concentrations of OH^-. At lower pH values, low-soluble hydroxides are precipitated, resulting in significantly lower metal concentrations. Especially in the case of Pb, the curve has a steep rise from pH 11 to 12.5, and the leaching concentrations increase here by four orders of magnitude. The leached amount of copper differs significantly between sample A and B. The reasons for this could be the higher Cu content in sample B (see Table 1) which, however, might not be systematic (inhomogeneity being observed especially for Cu and Zn, see above). Most likely, the reason for the difference is a higher concentration of dissolved organic carbon in the leachates (50–60 mg/kg for sample A, 100–140 mg/kg for sample B, both values calculated as leached amounts from TOC data in mg/L in both the batch and column experiments), resulting in enhanced copper complexation [48]. The influence of organic carbon, especially on copper complexation, has been intensively studied in the past [49–52]. However, it was outside the scope of the present study to include complexation reactions in the modelling of the experimental results. An almost linear dependence of the observed release of Cu as function of TOC is shown in the SI (Figure S1). The TOC dropped to lower values for the material stored outside compared to those from indoor storage.

The solid lines in Figure 3 for Cu, Zn, and Pb display the modelling results with the Visual MINTEQ program [37]. A rather simple modelling approach was selected. It was based on the leaching results at L/S = 10 L/kg for Cu, Zn, Pb, Sb, Ca, Na, sulfate, and chloride for dissolved species, and $Cu(OH)_2$, $PbCO_3$, $ZnCO_3$, Ca-antimonate, and ettringite as solid phases (entered as finite species in Vminteq, see SI Table S2). Solid phases tenorite (CuO), larnakite ($Pb_2(OH)_2SO_4$), and melanothallite (CuCl) were defined as excluded species because their presence in the model caused a failure of calculation at pH values 5.5 and 6.0. This has only a minor effect on the results because precipitation occurs mainly in the form of hydroxides, carbonates and (pure) sulfates. The Sweep function in the Vminteq program was applied to vary the pH from 3 to 13 in steps of 0.5 pH units. The respective hydroxo species of Cu and Zn were present in the integrated database thermo.vdb. Species $Pb(OH)_4^{2-}$ was not present and was therefore added, using the values for the stability constant from the MinteqA2 database MTQ3.11 (log K = −36.699) [38].

The leached amount at a pH of 4 is greater by at least one order of magnitude than the maximum values in the alkaline branch. Leaching at a fixed pH of 4 with maleic acid was included in the present study to compare leached amounts under "natural" conditions, i.e., from neutral to alkaline pH values to the acidic range, where the heavy metal release is significantly higher. However, the presence of maleic acid, i.e., possible complexation reactions with the organic ligand, was not included in the geochemical modelling with Visual MINTEQ. The solid lines in Figure 3 are almost horizontal in the pH range from 3 to 5 because the solid phases entered into the program were lower than the real concentrations in the samples.

The observed leaching results of Sb could not be modelled as function of pH with the applied simple approach. There is, therefore, no solid line in Figure 3d. The pH- dependent leaching of Sb is influenced by sorption on iron oxides and amorphous Al minerals, which are always present in IBA [53]. However, sorption was also not included in the model here. Nonetheless, precipitation was modelled by the addition of solid phase Ca-antimonate to the database, using a value for log K_s of −12.55 [54].

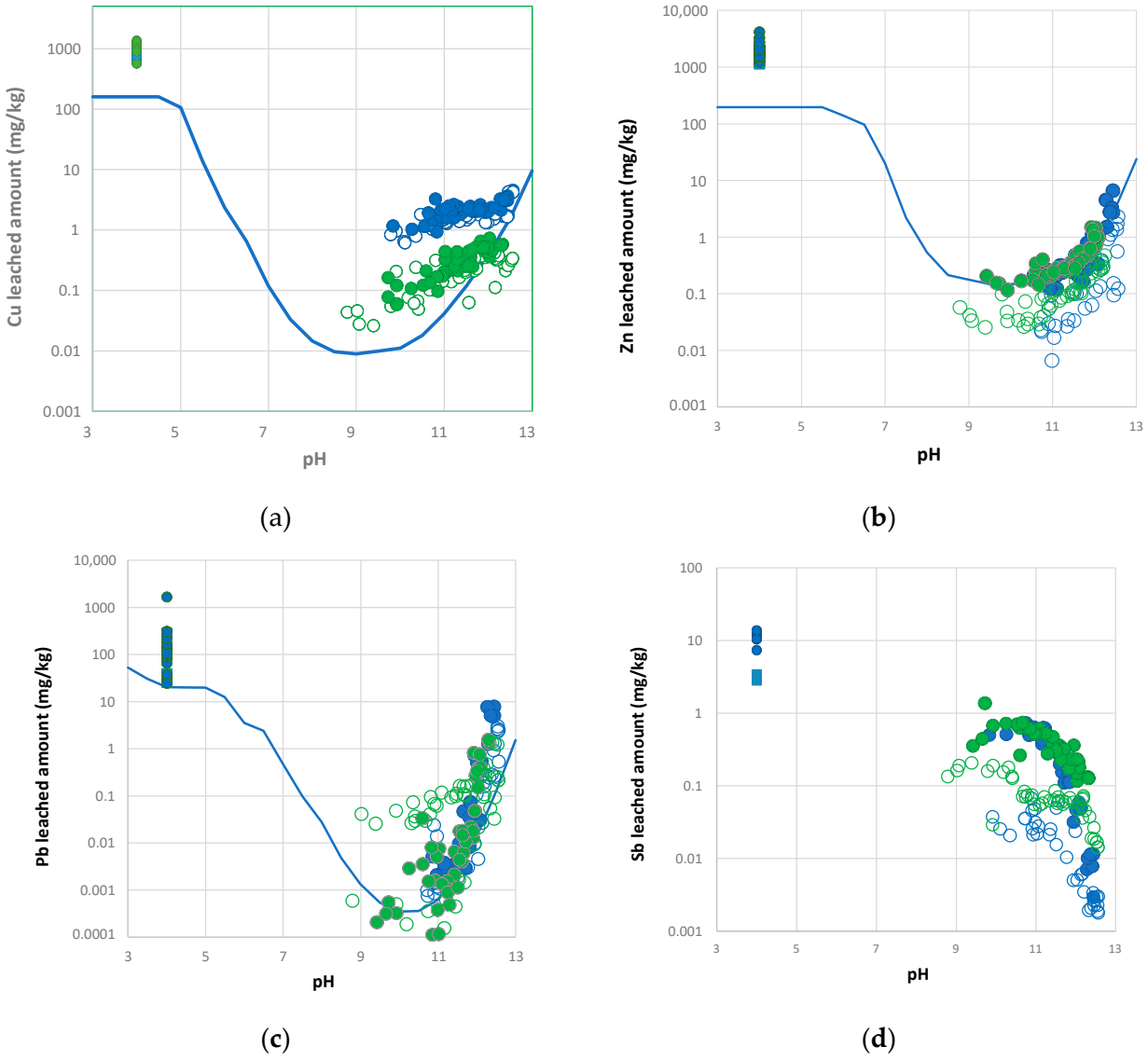

Figure 3. Leached amount (E) in mg/kg as a function of pH for the elements Cu (**a**), Zn (**b**), Pb (**c**), and Sb (**d**). Filled symbols are results at an L/S ratio of 10 L/kg, unfilled symbols at an L/S ratio of 2 L/kg. Green: sample A; blue: sample B.

Antimony (Sb) exists as the less toxic Sb(V) in IBA [55], i.e., specifically as oxyanion $Sb(OH)_6^-$ [27,56]. It shows a completely different dependence on pH from Cu, Zn, and Pb (see Figure 3d). In contrast, a correlation between the concentration of Ca and Sb was already found in landfill leachates in the 1990s [48]: high Sb concentration at low Ca concentration and vice versa, suggesting the precipitation of Sb(V) by Ca ions. The authors gave a stability constant log K = −15.5 for $Ca(Sb(OH)_6)_2$, changed in a later work to log K = −12.55 [54]. This finding was confirmed by various research groups [27,53,56] and was also reproduced in the present investigation, at least with the batch tests performed at an L/S ratio of 10 L/kg(see Figure 4). Here, the Ca concentrations were mostly in the narrow range between 100 and 250 mg/L (displayed as leached amount in mg/kg). In the batch tests with L/S = 2 L/kg, the data show more scattering. However, a reasonable agreement between the experimental data and the modelling results (Visual MINTEQ, using log K of Ca-antimonate = −12.55) was found, i.e., high Sb concentrations at low Ca concentration and vice versa.

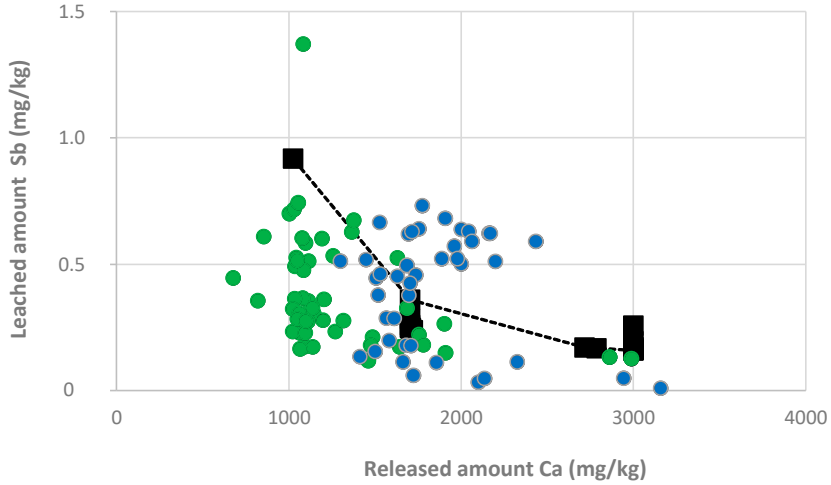

Figure 4. Leached amount of Sb as a function of Ca ions in batch test with L/S = 10 L/kg. Green: sample A; blue: sample B; black squares and dotted line: modelling results with Visual MINTEQ).

The leached amount of soluble components such as Na and Cl showed little variance with storage time and thus with the pH of the leachate. Large differences were observed, of course, between the samples with outdoor and indoor storage. Na and Cl dropped by more than 90% in sample A, which was stored outdoors (see Figure S2 in SI). The effect was much lower for sample B, due to less rainfall (factor 4: sample A 348 L/m^2, sample B 87.0 L/m^2), see the precipitation curve in Figure S2 in the SI.

The measured sulfate concentrations changed drastically during the course of the aging experiment, indicating that, at least in the beginning with fresh IBA, gypsum ($CaSO_4 \times 2\ H_2O$) is not the dominant phase present. For sample A, the sulfate concentrations were below 100 mg/L in the first 4 weeks in both standardized batch tests (i.e., leached amount <1000 mg/kg at L/S = 10 L/kg and <200 mg/kg at L/S = 2 L/kg), although the solubility of $CaSO_4$ is 2000 mg/L [26] (see Figure 5). This effect was also observed with sample B, but less pronouncedly. Maximum sulfate concentrations between 1300 and 1400 mg/L were observed after 10–12 weeks of storage time outdoors; the sulfate concentrations of the samples indoors did not exceed 1000 mg/L. Such low sulfate concentrations in leaching tests were also found in an Italian study of IBA in which the material from two of the five plants investigated showed low concentrations ranging between 5 and 47 mg/L at an L/S = 10 L/kg [57]. Meima and Comans found that the formation of ettringite in fresh IBA (formed from anhydrite in the unquenched state, i.e., before contact with water in the wet ash discharging system) may be responsible for this behavior [58]. Ettringite is a minimally soluble sulfate species ($Ca_6[Al(OH)_6]_2(SO_4)_3x26\ H_2O$ (log $K_L = -44.9$ [59,60]). At lower pH values (i.e., in batch tests with aged IBA), ettringite is no longer stable and other, more soluble Ca-sulfate species are formed [61].

The time-dependent behavior of sulfate can be observed even better in the column tests performed according to DIN 19529. In column tests, the respective concentrations in mg/L are measured at fixed L/S ratios, here at 0.3, 1, 2, 4, 7, and 10 L/kg. The leached amount determined in batch tests can be compared with the cumulative release of substances in a column test. First, the concentrations in the distinct leaching fractions are converted to leached amount (E_i) and then added together for the cumulative release U_i ($U_i = \Sigma\ E_i$). The maximum cumulative release of sulfate at L/S = 10 L/kg in the column experiment with fresh IBA was around 80 mg/kg (Figure 6b), whereas more than 1250 mg/kg was measured for the aged IBA sample (Figure 6d). The curves in Figure 6c,d can be explained by the presence of gypsum. In practice, the early transformation from ettringite to gypsum is not noticed because leaching tests are rarely performed with fresh bottom ash samples.

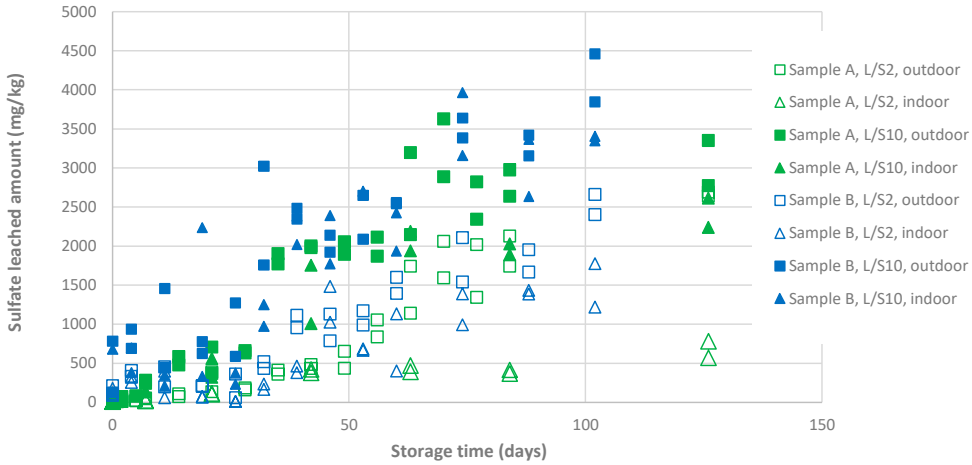

Figure 5. Sulfate concentration measured as a function of storage time in leaching tests at L/S = 2 L/kg and 10 L/kg with IBA samples A and B, stored outdoors and indoors. The sulfate concentrations are very low in the beginning (fresh IBA).

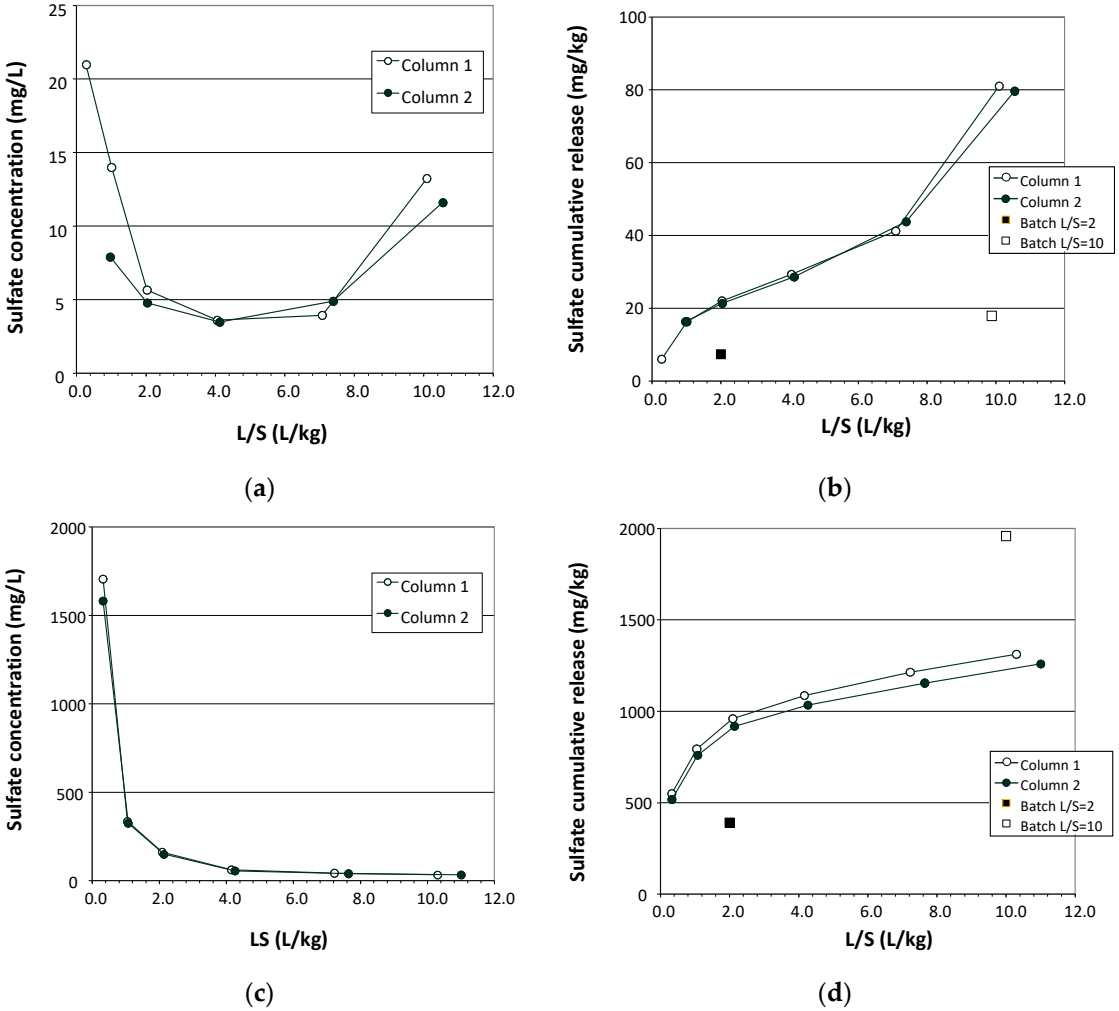

Figure 6. Measured concentrations (**a**) and calculated cumulative release U (**b**) of sulfate in fresh IBA (sample A) and after 84 days of indoor storage time (**c**,**d**, respectively). The results of the batch tests at L/S = 2 and 10 L/kg are drawn in the graphs (filled and unfilled squares) of cumulative release (**b**,**d**). Note the completely different scale of y-axes of (**a**,**b**) in comparison with (**c**,**d**).

The cumulative release for most heavy metals remains almost unchanged over the storage time (i.e., almost no difference between fresh and aged IBA), see the example of Cu in SI (Figure S4).

A reasonable agreement between batch and column tests was found for most analyzed components. Discrepancies are in the range of less than one order of magnitude, as shown in Figure 7 (numerical data in SI Table S2). As expected, the batch tests at the higher L/S ratio of 10 L/kg yielded slightly greater results for the leached amount than the batch tests at an L/S = 2 L/kg (see Figure S5 in the SI) simply due to the higher dilution factor.

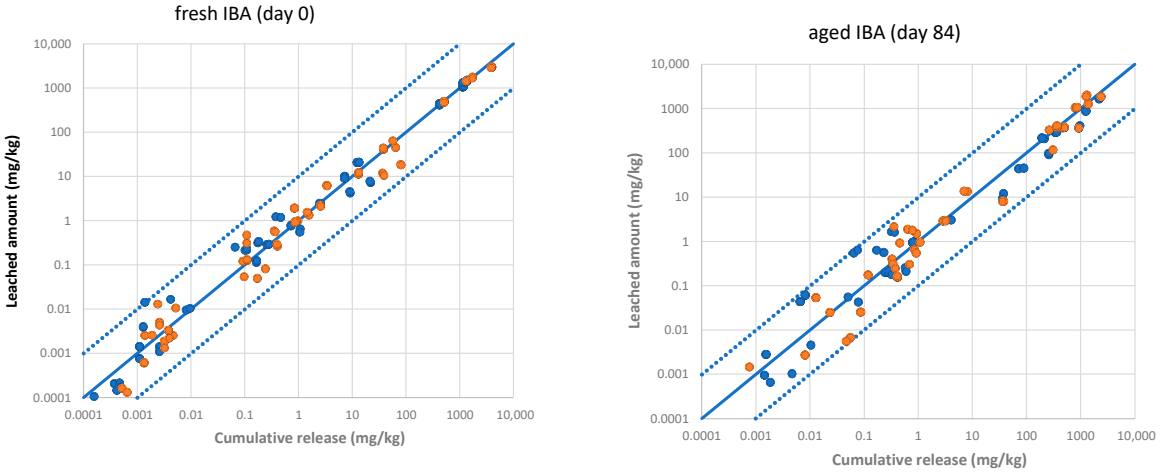

Figure 7. Comparison of batch test results (leached amount, *y*-axis) and column test results (cumulative release, *x*-axis) at L/S = 2 L/kg (blue symbols) and 10 L/kg (orange symbols). (**Left**): fresh IBA; (**Right**): IBA after 84 days of indoor storage.

4. Discussion and Conclusions

Incineration bottom ash consists of roughly 10% metals (Fe and NFe such as Cu, Cu alloys, and Al) and 90% mineral material. The recovery of the elemental metals has been improved over the years, so that the mineral fraction contains only traces of metal particles [8,15]. In Switzerland, there is a legal requirement to remove non-ferrous metals from IBA to less than 1% by weight [62]. The recovery of elemental metals is favorable economically due to achieved revenues and environmentally due to lower heavy metal content in the mineral fraction. In other European countries, including Germany, the recovery of NFe is common practice without being legally prescribed.

The remaining mineral material should be at least suitable for landfilling. In Germany, a first legal definition of requirements for landfilling of waste that cannot be otherwise used was the Technical Instruction Municipal Waste (TA Si), with two classes of landfills ("Deponieklasse I and II") [63]. Later, most of these limit values (defined for leaching tests with an L/S = 10 L/kg) were adopted into the German Ordinance on Landfills, with five classes (DK 0 for inert waste and DK I–IV for other waste) [64]. The requirements are mainly related to the leaching properties of IBA and are displayed for DK 0–II in Table 2. In the 1990s, it was unclear for operators of waste incineration plants whether IBA fulfills the requirements for Deponieklasse I, mainly due to the lack of appropriate studies of its leaching behavior. The limit value for Pb in TA Si was 0.2 mg/L. At that time, the storage of IBA to allow for the completion of the aging reactions described above before landfilling or use was not commonly established. Leaching tests with fresh bottom ash frequently yielded Pb concentrations around 1 mg/L, i.e., 10 mg/kg (L/S = 10 L/kg), as also observed in the present study (see Figure 3). However, it was rapidly recognized that the heavy metal concentrations decrease with the pH of the leachate as a result of the aging reactions [22]. This finding is confirmed with the results from the present study. The storage of IBA prior to landfilling or use, allowing alkaline earth oxides and hydroxides to react with CO_2, is a necessity to immobilize contaminants.

Table 2. Legal requirements for the use and landfilling of IBA. The limit values have been converted from concentrations to leached amounts because different leaching procedures are anticipated to check the requirements for use (HMVA-1 and-2: L/S = 2 L/kg) and landfilling (DK 0–II: L/S = 10 L/kg).

Parameter	Unit	HMVA-1	HMVA-2	DK 0	DK I	DK II
pH value	-	7–13	7–13	5.5–13	5.5–13	5.5–14
Electrical conductivity	µS/cm	2000	12,500			
DOC	mg/kg			500	800	1000
Cl	mg/kg	320	10,000	800	15,000	25,000
SO4	mg/kg	1640	6000	1000	20,000	20,000
Sb	µg/kg	20	120	60	300	700
Cr (total)	µg/kg	300	920	500	3000	10,000
Cu	µg/kg	220	2000	2000	10,000	50,000
Mo	µg/kg	110	800	500	3000	10,000
V	µg/kg	110	300			
As	µg/kg			500	2000	2000
Pb	µg/kg			500	2000	10,000
Cd	µg/kg			40	500	1000
Ni	µg/kg			400	2000	10,000
Hg	µg/kg			10	50	200
Zn	µg/kg			4000	20,000	50,000
Total dissolved matter	mg/kg			4000	30,000	60,000
TOC (solid content)	%			1	1	3

To save scarce landfill volume, today's aim in thermal waste treatment is to also use the mineral fraction of IBA. The most important use pathway of IBA is as secondary building material [47]. The requirements for the use of IBA in Europe were reviewed by Blasenbauer et al. [65]. Some countries have requirements on total content for certain parameters (e.g., TOC, loss on ignition, organic compounds), but usually the leaching behavior is decisive. Applied test procedures are mainly batch tests with L/S ratios of 2 and 10 L/kg and to a lesser extent percolation tests with L/S ratios from 0.1 to 10 L/kg. The limit values from the German Ordinance for Secondary Building Materials (defined for L/S = 2 L/kg) were implemented later (2021) and are listed in Table 2 for the material classes HMVA-1 and HMVA-2, with HMVA-1 enabling more permitted installation methods. For comparison, the limit values from the German Ordinance on Landfills are also listed (all values are converted to leached amount in µg/kg). It is commonly accepted that the results from batch tests at an L/S = 2 L/kg are closer to field conditions than those at an L/S = 10 L/kg [66]. Nevertheless, it was shown that the results are at least in the same order of magnitude.

It can be seen that the limit values for use according to HMVA-2 are less strict than the limit values for the inert landfill DK 0, although IBA is actually not classified as inert waste for DK 0. This is the case for most European countries except for Denmark and Sweden [14].

Our results reveal that IBA surely complies with the limit set for HMVA-2, but the quality requirements for HMVA-1 were not reached, mainly due to the parameters chloride and sulfate. The solid contents of chloride and sulfate are too high (see Table 1) and alkaline, and alkaline earth chlorides and even calcium sulfate exhibit higher solubilities than the allowed limits. As shown in the present study, ettringite with a low solubility is not stable in the course of the aging process and is transformed into other, more soluble calcium sulfate phases. The use of IBA as aggregate in concrete was studied (see e.g., [67]), but it is not well-developed in practice due to the presence of alkali salts, fine Al particles which could evolve hydrogen, and other disturbing substances. The main areas of application are landscaping (on landfill sites) and road construction, thus helping to save natural resources such as sand and gravel [47].

The geochemical modelling software Visual MINTEQ was able to predict the concentrations of relevant heavy metals in the leaching tests, as well as the precipitation of solids. Modelling complexation, as observed in the present study for copper, is also possible but

was not examined within the present study, along with sorption processes that are relevant for the release of Sb.

The leaching behavior of most heavy metals in IBA depends mainly on the pH of the leaching test. Antimonate (Sb-V) forms a stable mineral with Ca. Therefore, the mobilization of Sb depends on the concentration of Ca^{2+} ions, which is initially low due to the existence of ettringite and later, with the advancement of aging in IBA, due to the formation of $CaCO_3$ ($K_L = 1 \times 10^{-8}$ mol^2 L^{-2}). Nevertheless, IBA fulfills the requirements for landfilling and use for a variety of applications (e.g., the installation methods allowed for HMVA-2) after storage. Even aged IBA remains a reactive material. Demanding requirements such as Germany's HMVA-1, with low release of sulfate, chloride, and Sb, are not achievable. The exclusion of the fine fraction 0–2 mm (or 0–4 mm) where chloride and sulfate are enriched might be helpful to reach this goal. However, that would affect approximately 50% of the mass of IBA, which then might be disposed of on landfills. The problem of increasing Sb release as a result of decreasing Ca concentrations would still remain in such a scenario, especially in the long-term view, when most Ca is transformed into $CaCO_3$. A different approach could involve further thermal treatment of IBA, e.g., vitrification of IBA [68,69], which has, however, a high energy demand. There is still a need for further research on the improvement of the environmental compatibility of IBA.

Supplementary Materials: The following supporting information can be downloaded at: https://www.mdpi.com/article/10.3390/app132413228/s1, Figure S1: Measured release of copper as function of dissolved organic matter; Figure S2: Rain fallen (cumulative) during outdoor storage of samples A and B; Figure S3: Released amount in mg/kg of Na and Cl as function of pH. Released content of Cl as function of outdoor storage time and storage time indoor; Figure S4: Cumulative release of Cu in a column test as function of the L/S ratio, sample B, unaged and after 84 days storage time inside; Figure S5: Plot of leached amount in batch tests at L/S = 10 L/kg versus leached content at L/S = 2 L/kg; Table S1: pH values measured at the end of batch tests with samples stored outdoors and inside; Table S2: Input parameters for modelling with Visual MINTEQ; Table S3: Cumulative release (column test) and leached amount (batch test), respectively, in mg/kg for fresh (day 0) and aged (day 84) IBA sample A for various elements and anions.

Author Contributions: Conceptualization, F.-G.S.; methodology, F.-G.S. and P.S.; validation, F.-G.S.; investigation, P.S.; writing—original draft preparation, F.-G.S.; writing—review and editing, F.-G.S. and P.S.; project administration, P.S.; funding acquisition, F.-G.S. All authors have read and agreed to the published version of the manuscript.

Funding: This research was funded by German UMWELTBUNDESAMT (UBA's Refo-Plan 2020), grant number 3720333050.

Data Availability Statement: Data are available upon request from the corresponding author. The data are not publicly available due to privacy.

Acknowledgments: Experimental work was performed in part by Lucas Schröder. Chemical analyses and sample preparation were performed by Katja Nordhauß, Maren Riedel, Anna Böwe, and Bianca Coesfeld.

Conflicts of Interest: The authors declare no conflict of interest.

References

1. Kaza, S.; Yao, L.C.; Bhada-Tata, P.; Van Woerden, F. *What a Waste 2.0: A Global Snapshot of Solid Waste Management to 2050*; Urban Development Series Knowledge Papers; World Bank, Urban Development: Washington, DC, USA, 2018.
2. Williams, P.T. *Waste Treatment and Disposal*; John Wiley & Sons: West Sussex, UK, 1998.
3. Chandler, A.J.; Eighmy, T.T.; Hartlen, J.; Hjelmar, O.; Kosson, D.S.; Sawell, S.E.; van der Sloot, H.A.; Vehlow, J. (Eds.) *Municipal Solid Waste Incineration Residues, The International Ash Working Group*; Included in series Studies in Environmental Science; Elsevier: Amsterdam, The Netherlands, 1997; Volume 67.
4. Bayuseno, A.P.; Schmahl, W.W. Understanding the chemical and mineralogical properties of the inorganic portion of MSWI bottom ash. *Waste Manag.* **2010**, *30*, 1509–1520. [CrossRef] [PubMed]
5. Huber, F.; Blasenbauer, D.; Aschenbrenner, P.; Fellner, J. Complete determination of the material composition of municipal solid waste incineration bottom ash. *Waste Manag.* **2020**, *102*, 677–685. [CrossRef] [PubMed]

6. Huber, F.; Korotenko, E.; Šyc, M.; Fellner, J. Material and chemical composition of municipal solid waste incineration bottom ash fractions with different densities. *J. Mater. Cycles Waste Manag.* **2020**, *23*, 394–401. [CrossRef]
7. van de Wouw, P.; Loginova, E.; Florea, M.; Brouwers, H. Compositional modelling and crushing behaviour of MSWI bottom ash material classes. *Waste Manag.* **2020**, *101*, 268–282. [CrossRef]
8. Šyc, M.; Simon, F.G.; Hykš, J.; Braga, R.; Biganzoli, L.; Costa, G.; Funari, V.; Grosso, M. Metal recovery from incineration bottom ash: State-of-the-art and recent developments. *J. Hazard. Mater.* **2020**, *393*, 122433. [CrossRef] [PubMed]
9. Wei, Y.; Shimaoka, T.; Saffarzadeh, A.; Takahashi, F. Mineralogical characterization of municipal solid waste incineration bottom ash with an emphasis on heavy metal-bearing phases. *J. Hazard. Mater.* **2011**, *187*, 534–543. [CrossRef] [PubMed]
10. Hyks, J.; Astrup, T. Influence of operational conditions, waste input and ageing on contaminant leaching from waste incinerator bottom ash: A full-scale study. *Chemosphere* **2009**, *76*, 1178–1184. [CrossRef]
11. Meima, J.A.; Comans, R.N.J. Overview of Geochemical Processes Controlling Leaching Characteristics of MSWI Bottom Ash. In *Studies in Environmental Science*; Goumans, J.J.J.M., Senden, G.J., van der Sloot, H.A., Eds.; Elsevier: Amsterdam, The Netherlands, 1997; Volume 71, pp. 447–457. [CrossRef]
12. Speiser, C.; Baumann, T.; Niessner, R. Characterization of municipal solid waste incineration (MSWI) bottom ash by scanning electron microscopy and quantitative energy dispersive X-ray microanalysis (SEM/EDX). *Anal. Bioanal. Chem.* **2001**, *370*, 752–759. [CrossRef]
13. Quina, M.J.; Bontempi, E.; Bogush, A.; Schlumberger, S.; Weibel, G.; Braga, R.; Funari, V.; Hyks, J.; Rasmussen, E.; Lederer, J. Technologies for the management of MSW incineration ashes from gas cleaning: New perspectives on recovery of secondary raw materials and circular economy. *Sci. Total. Environ.* **2018**, *635*, 526–542. [CrossRef]
14. Blasenbauer, D.; Huber, F.; Lederer, J.; Quina, M.J.; Blanc-Biscarat, D.; Bogush, A.; Bontempi, E.; Blondeau, J.; Chimenos, J.M.; Dahlbo, H.; et al. Legal situation and current practice of waste incineration bottom ash utilisation in Europe. *Waste Manag.* **2020**, *102*, 868–883. [CrossRef]
15. Holm, O.; Simon, F.-G. Innovative treatment trains of bottom ash (BA) from municipal solid waste incineration (MSWI) in Germany. *Waste Manag.* **2017**, *59*, 229–236. [CrossRef]
16. Bunge, R. Recovery of Metals from Waste Incineration Bottom Ash. In *Removal, Treatment and Utilisation of Waste Incineration Bottom Ash*; Holm, O., Thome-Kozmiensky, E., Eds.; TK Verlag: Neuruppin, Germany, 2018; pp. 63–143.
17. Astrup, T.; Muntoni, A.; Polettini, A.; Pomi, R.; Van Gerven, T.; Van Zomeren, A. Treatment and Reuse of Incineration Bottom Ash. In *Environmental Materials and Waste, Resource Recovery and Pollution Prevention*; Prasad, M.N.V., Shih, K., Eds.; Academic Press: Amsterdam, The Netherlands, 2016; pp. 607–645. [CrossRef]
18. Kahle, K.; Kamuk, B.; Kallesøe, J.; Fleck, E.; Lamers, F.; Jacobsson, L.; Sahlén, J. *Bottom Ash from WtE Plants, Metal Recovery and Utilization, Report*; International Solid Waste Association ISWA: Vienna, Italy, 2015.
19. Chen, B.; Perumal, P.; Illikainen, M.; Ye, G. A review on the utilization of municipal solid waste incineration (MSWI) bottom ash as a mineral resource for construction materials. *J. Build. Eng.* **2023**, *71*, 106386. [CrossRef]
20. Di Gianfilippo, M.; Hyks, J.; Verginelli, I.; Costa, G.; Hjelmar, O.; Lombardi, F. Leaching behaviour of incineration bottom ash in a reuse scenario: 12 years-field data vs. lab test results. *Waste Manag.* **2018**, *73*, 367–380. [CrossRef] [PubMed]
21. Hyks, J.; Syc, M. Utilisation of Incineration Bottom Ash in Road Construction. In *Waste Mangement*; Thiel, S., Thomé-Kozmiensky, E., Winter, F., Juchelkova, D., Eds.; Waste-to-Energy, TK-Verlag: Nietwerder, Germany, 2019; Volume 9, pp. 731–741.
22. Simon, F.G.; Schmidt, V.; Carcer, B. Alterungsverhalten von MVA-Schlacken. *Müll Abfall* **1995**, *27*, 759–764.
23. Krüger, O.; Kalbe, U.; Berger, W.; Simon, F.-G.; Meza, S.L. Leaching experiments on the release of heavy metals and PAH from soil and waste materials. *J. Hazard. Mater.* **2012**, *207–208*, 51–55. [CrossRef] [PubMed]
24. Meza, S.L.; Kalbe, U.; Berger, W.; Simon, F.-G. Effect of contact time on the release of contaminants from granular waste materials during column leaching experiments. *Waste Manag.* **2010**, *30*, 565–571. [CrossRef]
25. Liu, B.; Finkel, M.; Grathwohl, P. Mass Transfer Principles in Column Percolation Tests: Initial Conditions and Tailing in Heterogeneous Materials. *Materials* **2021**, *14*, 4708. [CrossRef]
26. Rauscher, K.; Voigt, J.; Wilke, I.; Wilke, K.T. *Chemische Tabellen und Rechentafeln für die Analytische Praxis*, 6th ed.; VEB Deutscher Verlag für Grundstoffindustrie: Leipzig, Germany, 1977.
27. Simon, F.-G.; Vogel, C.; Kalbe, U. Antimony and vanadium in incineration bottom ash—Leaching behavior and conclusions for treatment processes. *Detritus* **2021**, *16*, 75–81. [CrossRef]
28. Bandarra, B.S.; Silva, S.; Pereira, J.L.; Martins, R.C.; Quina, M.J. A Study on the Classification of a Mirror Entry in the European List of Waste: Incineration Bottom Ash from Municipal Solid Waste. *Sustainability* **2022**, *14*, 10352. [CrossRef]
29. Bandarra, B.; Mesquita, C.; Passos, H.; Martins, R.; Coelho, P.; Pereira, J.; Quina, M. An integrated characterisation of incineration bottom ashes towards sustainable application: Physicochemical, ecotoxicological, and mechanical properties. *J. Hazard. Mater.* **2023**, *455*, 131649. [CrossRef]
30. Dijkstra, J.J.; A van der Sloot, H.; Comans, R.N. Process identification and model development of contaminant transport in MSWI bottom ash. *Waste Manag.* **2002**, *22*, 531–541. [CrossRef] [PubMed]
31. Piantone, P.; Bodénan, F.; Chatelet-Snidaro, L. Mineralogical study of secondary mineral phases from weathered MSWI bottom ash: Implications for the modelling and trapping of heavy metals. *Appl. Geochem.* **2004**, *19*, 1891–1904. [CrossRef]
32. Dijkstra, J.J.; Van Der Sloot, H.A.; Comans, R.N. The leaching of major and trace elements from MSWI bottom ash as a function of pH and time. *Appl. Geochem.* **2006**, *21*, 335–351. [CrossRef]

33. Dijkstra, J.J.; Meeussen, J.C.; Van der Sloot, H.A.; Comans, R.N. A consistent geochemical modelling approach for the leaching and reactive transport of major and trace elements in MSWI bottom ash. *Appl. Geochem.* **2008**, *23*, 1544–1562. [CrossRef]
34. Di Gianfilippo, M.; Costa, G.; Verginelli, I.; Gavasci, R.; Lombardi, F. Analysis and interpretation of the leaching behaviour of waste thermal treatment bottom ash by batch and column tests. *Waste Manag.* **2016**, *56*, 216–228. [CrossRef]
35. Huber, F.; Blasenbauer, D.; Aschenbrenner, P.; Fellner, J. Chemical composition and leachability of differently sized material fractions of municipal solid waste incineration bottom ash. *Waste Manag.* **2019**, *95*, 593–603. [CrossRef] [PubMed]
36. Luo, H.; Cheng, Y.; He, D.; Yang, E.-H. Review of leaching behavior of municipal solid waste incineration (MSWI) ash. *Sci. Total. Environ.* **2019**, *668*, 90–103. [CrossRef] [PubMed]
37. Gustafsson, J.P. *Visual MINTEQ, a Freeware Chemical Equilibrium Model for the Calculation of Metal Speciation, Solubility Equilibria, Sorption etc. for Natural Waters*; Version 3.1; 2020; Available online: https://vminteq.lwr.kth.se/ (accessed on 10 December 2023).
38. Allison, J.D.; Brown, D.S.; Novo-Gradac, K.J. *MinteqA2/ProdefA2, A Geochemical Assessment Model for Environmental Systems, Database of Computer Programme*; Version 3.0; US Environmental Protection Agency: Athens, GA, USA, 1991.
39. *DIN 19529: 2015-12*; Elution von Feststoffen—Schüttelverfahren zur Untersuchung des Elutionsverhaltens von anorganischen und organischen Stoffen mit einem Wasser/Feststoff-Verhältnis von 2 l/kg. Beuth-Verlag: Berlin, Germany, 2015.
40. *DIN EN 12457-2: 2003-01*; Charakterisierung von Abfällen—Auslaugung; Übereinstimungsuntersuchung für die Auslaugung von körnigen Abfällen und Schlämmen—Teil 2: Einstufiges Schüttelverfahren mit einem Flüssigkeits-/Feststoffverhältnis von 10 l/kg und einer Korngröße unter 4 mm (ohne oder mit Korngrößenreduzierung). Beuth-Verlag: Berlin, Germany, 2003.
41. *DIN 19528: 2009-01*; Elution von Feststoffen—Perkolationsverfahren zur gemeinsamen Untersuchung des Elutionsverhaltens von organischen und anorganischen Stoffen für Materialien mit einer Korngröße bis 32 mm—Grundlegende Charakterisierung mit einem ausführlichen Säulenversuch und Übereinstimmungsuntersuchung mit einem Säulenschnelltest. Beuth-Verlag: Berlin, Germany, 2009.
42. *DIN ISO 11466:1997-06*; Bodenbeschaffenheit—Extraktion in Königswasser löslicher Spurenelemente (Soil Quality—Extraction of Trace Elements Soluble in Aqua Regia). Beuth-Verlag: Berlin, Germany, 1997.
43. Hennebert, P. Hazard Classification of Waste: Review of Available Practical Methods and Tools. *Detritus* **2019**, *7*, 13–28. [CrossRef]
44. IGAM; ITAD. *Einstufung von Hausmüllverbrennungsschlacken in das Abfallverzeichnis Anhand der Gefahrenrelevanten Eigenschaften HP1-HP15, Praxisleitfaden der Verbände IGAM und ITAD e.V.*; Version 2.0 vom 18.06.2019; 2019; Available online: https://www.itad.de/service/mitgliederinfos/oeffentliche-anhaenge/20200424-praxisleitfaden_igam-itad-zur-einstufung-von-hmv-schlacke_version_2-1.pdf (accessed on 10 December 2023).
45. Nordsieck, H.; Wambach, K.; Thiel, N.; Warnecke, R.; Rommel, W. Gefährliche Eigenschaft HP14 von Rostaschen. In *Mineralische Nebenprodukte und Abfälle, Aschen, Schlacken Stäube und Baurestmassen*; Thiel, S., Thomé-Kozmiensky, E., Pretz, T., Senk, D.G., Wotruba, H., Eds.; TK-Verlag: Neuruppin, Germany, 2019; Volume 6, pp. 98–112.
46. Hjelmar, O.; van der Sloot, H.A.; van Zomeren, A. Hazard property classification of high temperature waste materials. In Proceedings of the Fourteenth International Waste Management and Landfill Symposium, S. Margerita di Pula, Cagliari, Italy, 30 September–4 October 2013; CISA Publisher: Padova, Italy, 2013.
47. Simon, F.-G.; Kalbe, U. Case Study on Secondary Building Materials for a Greener Economy. *Appl. Sci.* **2023**, *13*, 6010. [CrossRef]
48. Johnson, C.; Kaeppeli, M.; Brandenberger, S.; Ulrich, A.; Baumann, W. Hydrological and geochemical factors affecting leachate composition in municipal solid waste incinerator bottom ash: Part II. The geochemistry of leachate from Landfill Lostorf, Switzerland. *J. Contam. Hydrol.* **1999**, *40*, 239–259. [CrossRef]
49. Arickx, S.; De Borger, V.; Van Gerven, T.; Vandecasteele, C. Effect of carbonation on the leaching of organic carbon and of copper from MSWI bottom ash. *Waste Manag.* **2010**, *30*, 1296–1302. [CrossRef]
50. Meima, J.A.; van Zomeren, A.; Comans, R.N.J. Complexation of Cu with dissolved organic carbon in municipal solid waste incinerator bottom ash leachates. *Environ. Sci. Technol.* **1999**, *33*, 1424–1429. [CrossRef]
51. Olsson, S.; van Schaik, J.W.J.; Gustafsson, J.P.; Kleja, D.B.; van Hees, P.A.W. Copper(II) Binding to Dissolved Organic Matter Fractions in Municipal Solid Waste Incinerator Bottom Ash Leachate. *Environ. Sci. Technol.* **2007**, *41*, 4286–4291. [CrossRef] [PubMed]
52. van Zomeren, A.; Comans, R.N.J. Contribution of Natural Organic Matter to Copper Leaching from Municipal Solid Waste Incinerator Bottom Ash. *Environ. Sci. Technol.* **2004**, *38*, 3927–3932. [CrossRef] [PubMed]
53. Cornelis, G.; Van Gerven, T.; Vandecasteele, C. Antimony leaching from MSWI bottom ash: Modelling of the effect of pH and carbonation. *Waste Manag.* **2012**, *32*, 278–286. [CrossRef] [PubMed]
54. Johnson, C.A.; Moench, H.; Wersin, P.; Kugler, P.; Wenger, C. Solubility of Antimony and Other Elements in Samples Taken from Shooting Ranges. *J. Environ. Qual.* **2005**, *34*, 248–254. [CrossRef] [PubMed]
55. Okkenhaug, G.; Almås, Å.R.; Morin, N.; Hale, S.E.; Arp, H.P.H. The presence and leachability of antimony in different wastes and waste handling facilities in Norway. *Environ. Sci. Process. Impacts* **2015**, *17*, 1880–1891. [CrossRef] [PubMed]
56. Kalbe, U.; Simon, F.-G. Potential Use of Incineration Bottom Ash in Construction: Evaluation of the Environmental Impact. *Waste Biomass-Valorization* **2020**, *11*, 7055–7065. [CrossRef]
57. Mantovani, L.; De Matteis, C.; Tribaudino, M.; Boschetti, T.; Funari, V.; Dinelli, E.; Toller, S.; Pelagatti, P. Grain size and mineralogical constraints on leaching in the bottom ashes from municipal solid waste incineration: A comparison of five plants in northern Italy. *Front. Environ. Sci.* **2023**, *11*, 1179272. [CrossRef]

58. Meima, J.A.; Comans, R.N.J. Geochemical Modeling of Weathering Reactions in Municipal Solid Waste Incinerator Bottom Ash. *Environ. Sci. Technol.* **1997**, *31*, 1269–1276. [CrossRef]
59. Perkins, R.B.; Palmer, C.D. Solubility of ettringite ($Ca_6[Al(OH)_6]_2(SO_4)_3 \cdot 26H_2O$) at 5–75 °C. *Geochim. Cosmochim. Acta* **1999**, *63*, 1969–1980. [CrossRef]
60. Warren, C.; Reardon, E. The solubility of ettringite at 25°C. *Cem. Concr. Res.* **1994**, *24*, 1515–1524. [CrossRef]
61. Myneni, S.C.; Traina, S.J.; Logan, T.J. Ettringite solubility and geochemistry of the $Ca(OH)_2$–$Al_2(SO_4)_3$–H_2O system at 1 atm pressure and 298 K. *Chem. Geol.* **1998**, *148*, 1–19. [CrossRef]
62. Schweizerischer Bundesrat. *Verordnung über Die Vermeidung und Die Entsorgung von Abfällen (VVEA)*; 2015; Available online: https://www.fedlex.admin.ch/eli/cc/2015/891/de (accessed on 10 December 2023).
63. Bundesregierung. TA Siedlungsabfall, Technische Anleitung zur Verwertung, Behandlung und Sonstigen Entsorgung von Siedlungsabfällen (Dritte Allgemeine Verwaltungsvorschrift zum Abfallgesetz) vom 14. Mai 1993, Bundesanzeiger 99a. 1993. Available online: https://www.lanuv.nrw.de/fileadmin/lanuv/abfall/tasi.pdf (accessed on 10 December 2023).
64. Bundesregierung. Verordnung über Deponien und Langzeitlager (Deponieverordnung—DepV), Bundesgesetzblatt I (2002) 2807. 2002. Available online: https://www.gesetze-im-internet.de/depv_2009/DepV.pdf (accessed on 10 December 2023).
65. Blasenbauer, D.; Huber, F.; Lederer, J.; Fellner, J. Utilisation of Incineration Bottom Ash and Respective Legal Requirements in the EU, Norway and Switzerland. In *Waste Mangement*; Thiel, S., Thomé-Kozmiensky, E., Winter, F., Juchelkova, D., Eds.; Waste-to-Energy, TK-Verlag: Nietwerder, Germany, 2019; Volume 9, pp. 715–729.
66. Eberle, S.H.; Freyas, R.; Huckele, S.; Haag, I.; Rödelsperger, M. *Sickerwasserprognose, Forschungsreport (Schlussbericht), 02WA0071*; Heinrich-Sontheimer-Laboratorium im Technologiezentrum Wasser: Karlsruhe, Germany, 2010.
67. Lynn, C.J.; Obe, R.K.D.; Ghataora, G.S. Municipal incinerated bottom ash characteristics and potential for use as aggregate in concrete. *Constr. Build. Mater.* **2016**, *127*, 504–517. [CrossRef]
68. Stabile, P.; Bello, M.; Petrelli, M.; Paris, E.; Carroll, M. Vitrification treatment of municipal solid waste bottom ash. *Waste Manag.* **2019**, *95*, 250–258. [CrossRef]
69. Xiao, Y.; Oorsprong, M.; Yang, Y.; Voncken, J. Vitrification of bottom ash from a municipal solid waste incinerator. *Waste Manag.* **2008**, *28*, 1020–1026. [CrossRef]

Supporting Information

Assessment of the long-term leaching behavior of incineration bottom ash: a study of two waste incinerators in Germany

Franz-Georg Simon [a, *] and Philipp Scholz [a]

[a] *BAM Bundesanstalt für Materialforschung und -prüfung, Division Contaminant Transfer and Environmental Technologies, 12200 Berlin, Germany*

* Corresponding author.
E-Mail address: franz-georg.simon@bam.de (F. G. Simon), BAM Bundesanstalt für Materialforschung und -prüfung, Berlin, Germany

Table S1. pH values measured at the end of batch tests with samples stored outdoor and inside.

Sample A				**Sample B**			
	Time (days)	pH (L/S 10)	pH (L/S 2)		Time (days)	pH (L/S 10)	pH (L/S 2)
outdoor	0	12.32	12.53	**outdoor**	0	12.44	12.53
	1	11.92	12.39		4	12.27	12.56
	2	12.03	12.34		11	11.94	12.32
	5	12.07	12.19		19	11.65	12.03
	7	11.95	12.04		26	11.59	11.51
	14	11.86	11.93		32	11.43	11.37
	21	11.6	11.54		39	11.15	11.06
	28	11.61	11.68		46	10.96	10.72
	35	11.42	11.45		53	10.86	10.73
	42	11.23	11.21		60	10.73	10.6
	49	11.31	11.16		74	10.55	10.09
	56	10.92	10.71		88	10.75	10.29
	63	11.03	10.74		102	9.83	9.91
	70	10.59	10.18				
	77	10.52			0	12.41	12.54
	84	10.25	9.92		4	12.29	12.46
	126	9.72			11	12.08	12.45
	281	9.42	8.79		19	11.81	12.2
					26	11.71	11.77
	0	12.3	12.55		32	11.38	11.34
	1	12.03	12.46		39	11.23	11.03
	2	11.96	12.45		46	11.23	10.98
	5	12.09	12.17		53	10.92	10.7
	7	11.94	12.14		60	10.95	10.58
	14	11.83	12.09		74	10.83	10.35
	21	11.9	11.74		88	10.26	10.1
	28	11.55	11.56		102	10.15	9.78
	35	11.42	11.34				

Sample A				Sample B			
	Time (days)	pH (L/S 10)	pH (L/S 2)		Time (days)	pH (L/S 10)	pH (L/S 2)
	42	11.1	10.9	**inside**	0		
	49	11.24	10.96		4	12.44	12.54
	56	10.99	10.79		11	12	12.38
	63	10.96	10.67		19	11.82	12.13
	70	10.83	10.4		26	11.83	11.99
	77	10.85	10.41		32	11.66	11.57
	84	10.67	10.31		39	11.19	10.89
	126	9.92	9.39		46	11.17	10.93
	281	9.66	9.02		53		10.6
					60	11.32	11.13
inside	0	12.32	12.53		74	11.1	10.87
	7	12.03	12.16		88	11.06	10.71
	21	11.65	12.19		102	10.64	10.64
	42	11.71	11.85				
	63	11.63	11.66		0		
	84	11.51	11.48		4	12.36	12.56
	126	11.29	11.09		11	12.12	12.43
	281	10.6	9.91		19	11.84	12.16
					26	11.81	11.94
	0	12.3	12.55		32	11.54	11.51
	7	12	12.24		39	11.17	10.97
	21	11.9	12.14		46	11.22	10.91
	42	11.55	11.66		53	11.16	10.9
	63	11.63	11.69		60	11.11	10.83
	84	11.54	11.46		74	10.93	10.61
	126	11.02	10.81		88	11.01	10.67
	281	10.76	10.35		102	10.8	10.46

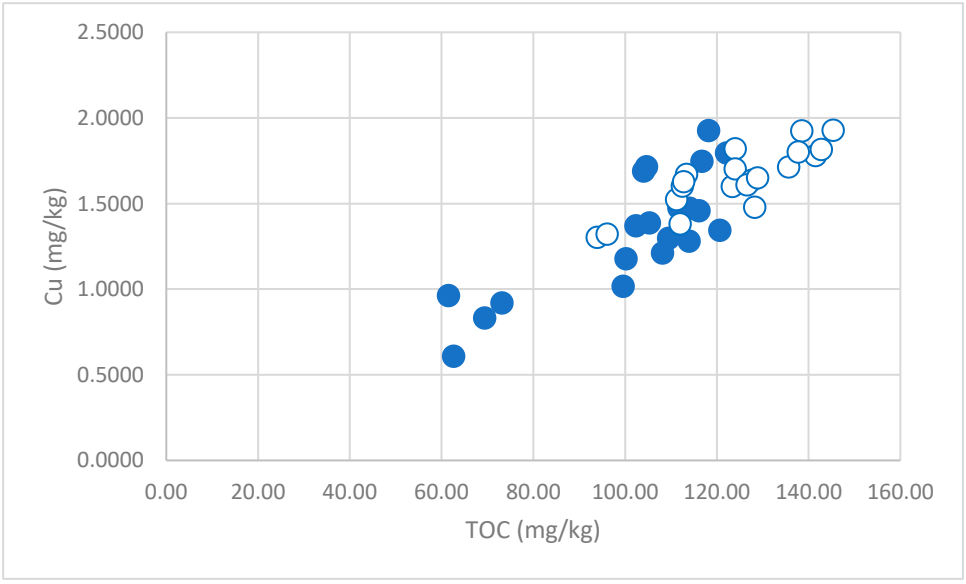

Figure S1. Measured release of copper as function of dissolved organic matter (sample B, L/S=2 L/kg, filled circles outdoor, unfilled circles indoor)

Table S2. Input parameters for modelling with Visual MINTEQ

Input		Debye-Hückel activity correction				
L/S=10 L/kg						
in solution	M (g/mol)	in solution	in solid	n(solv.)	n(solid)	sum
		mg/L	mg/0.1 kg			
Cu	63.6	0.05	150	7.86164E-07	0.00235849	2.36E-03
Zn	65.4	0.2	200	3.0581E-06	0.0030581	3.06E-03
Pb	207.2	0.1	50	4.82625E-07	0.00024131	2.42E-04
Sb	121.8	0.05	10	4.10509E-07	8.2102E-05	8.25E-05
Na	23	200		0.008695652	0	8.70E-03
Cl	35.5	650		0.018309859	0	1.83E-02
Ca	40	300		0.0075	0	7.50E-03
SO4	96	200		0.002083333	0	2.08E-03
Al	27	10	1500	3.70E-04	0.05555556	5.59E-02

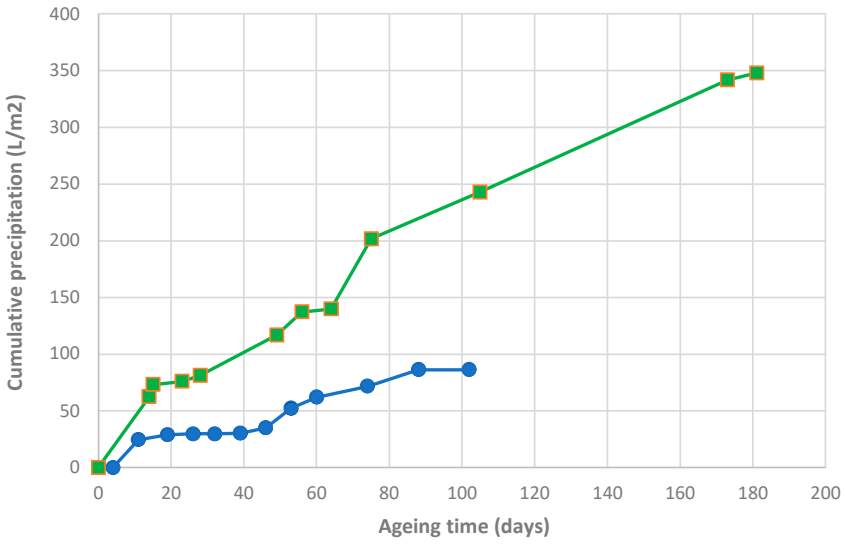

Figure S2. Rain fallen (cumulative) during outdoor storage of samples A (green squares) and B (blue circles).

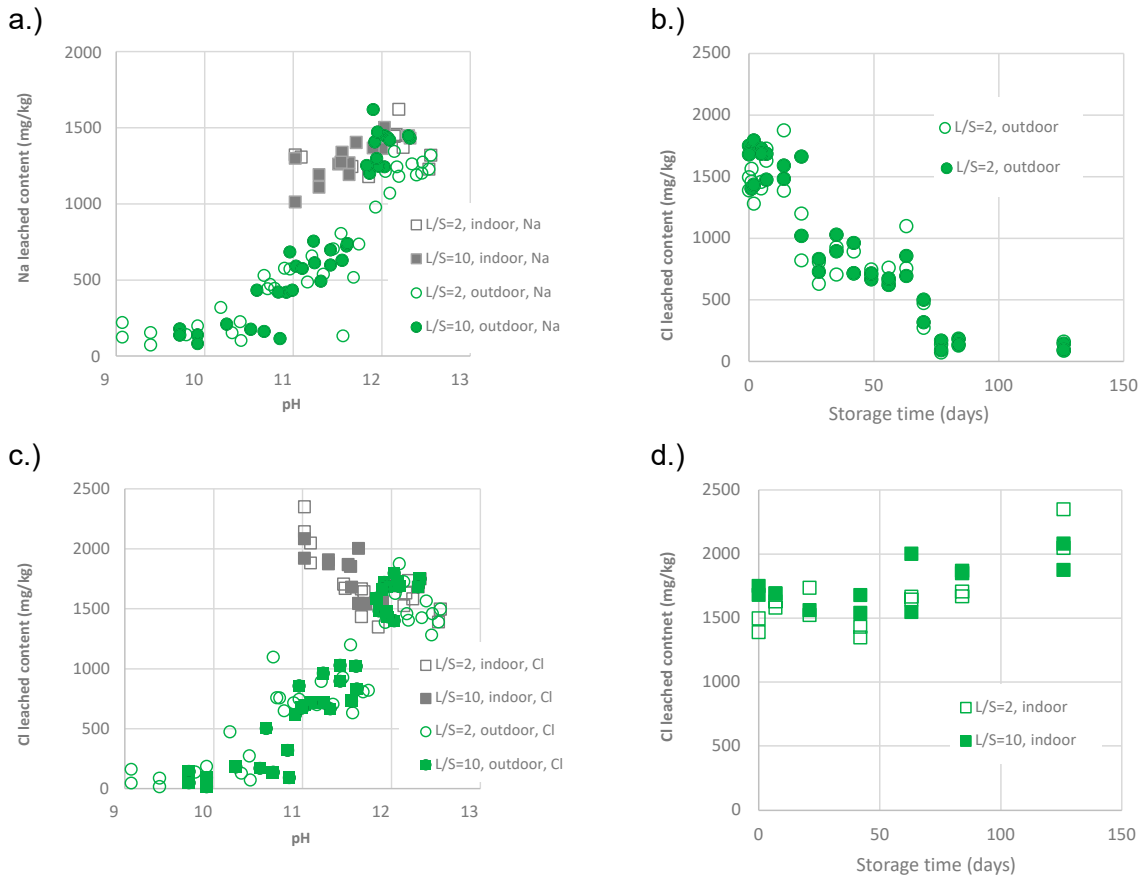

Figure S3. Released amount in mg/kg of Na (a) and Cl (b) as function of pH. The results from the samples stored indoor show that there is no pH dependence. Decreasing values are the result of wash out by rainfall. Released content of Cl as function of outdoor storage time (c) and storage time indoor (d). All results are from sample A.

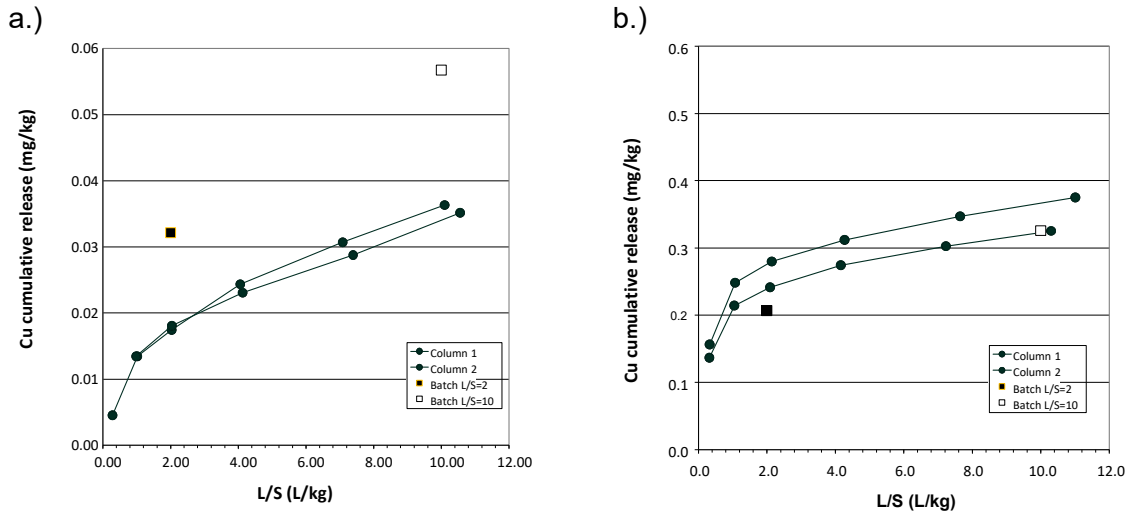

Figure S4. Cumulative release of Cu in a column test as function of the L/S ratio, sample B, unaged (a) and after 84 days storage time inside (b). The release is in both cases in the range of 400 µg/kg.

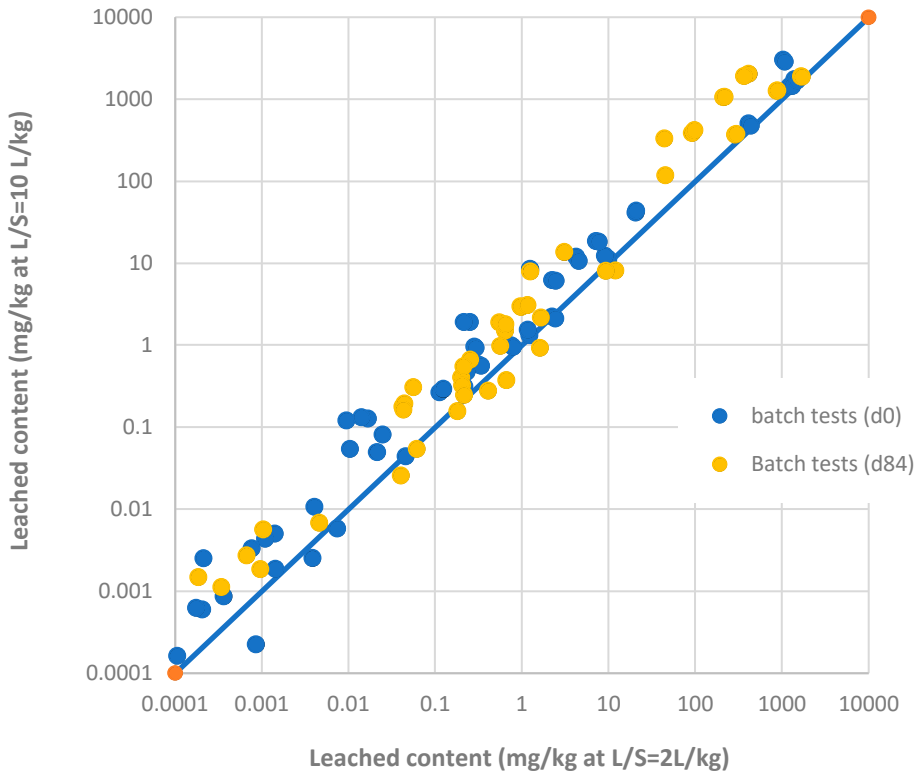

FigureS5. Plot of leached amount in batch tests at L/S=10 L/kg versus leached content at L/S=2 L/kg.

Table S3. Cumulative release (column test) resp. leached amount (batch test) in mg/kg for fresh (day 0) and aged (day 84) IBA sample A for various elements and anions. Duplicate analysis (1: lines 1-36, 2: lines 38-73).

Sample A		**Fresh (day 0)**				**Aged (day 84)**			
Parameter	**Unit**	**Column test**		**Batch test**		**Column test**		**Batch test**	
L/S	**L/kg**	**2**	**10**	**2**	**10**	**2**	**10**	**2**	**10**
As	mg/kg	0.00037449	0.00132958	0.00020626	0.0005998	0.00141082	0.01012052		
Ba	mg/kg	12.2004207	38.0219023	20.5917296	41.0761715	0.06402664	0.63576784	0.5495898	1.89186953
Cd	mg/kg	0	0			2.8941E-05	0.00075822	0.00018497	0.00147812
Cr	mg/kg	0.00812208	0.09167033	0.00957194	0.12104262	0.57656589	0.84787879	0.25460618	0.66268537
Cu	mg/kg	0.17459486	0.35145439	0.31462205	0.57865404	0.2414226	0.32531102	0.19931991	0.40434546
Hg	mg/kg	0.00046377	0.00138102	0.00021262	0.00252614	0.00143914		0.00095835	0.0018575
Mn	mg/kg	0	0.00187801		0.00258855	0.00084349	0.0084969		
Mo	mg/kg	0.16433013	0.40423548	0.11235153	0.26605172	0.26768255	0.33972805	0.20479069	0.3229046
Ni	mg/kg	0.00257616	0.00257616	0.0014161	0.00506795	0.00126838	0.02337609		0.02504946
Pb	mg/kg	0.37717028	1.56819879	1.22107774	1.33019455	0	0.01532818		
Sb	mg/kg	0.00414342	0.11139327	0.01672522	0.12676181	0.05067979	0.68996408	0.0559901	0.30550111
Sn	mg/kg	0.00128347	0.00467475	0.00388802	0.00253332	0.01040572	0.05575033	0.0045804	0.00682421
Sr	mg/kg	7.23490919	13.0085007	9.99307075	11.2581648	0.82841128	2.86772486	0.9784569	2.91676506
V	mg/kg	0.00015093	0.00322112			0.01104408	0.03994021		
Zn	mg/kg	0.06548638	0.83622878	0.25122232	1.91001495	0	0.11824122	0.04218758	0.17676207
Co	mg/kg	0.00015641	0.00052012	0.00010605	0.00016232	0.00066843	0.00434261		
Al	mg/kg	1.07339597	63.9628078	0.65075238	45.0130154	71.4018127	261.766398	44.0027411	332.496517
Ca	mg/kg	1136.48215	3954.96799	1036.27357	2987.95961	212.389279	798.573316	209.80507	1059.51146
Fe	mg/kg	0	0	0.0008633	0.00022422	0	37.5332278		
K	mg/kg	417.969435	509.875039	407.975941	503.361271	343.828825	475.191407	289.262242	369.198697
Mg	mg/kg	0	0	0.00746053	0.00581852	0.09514308	0.09514308		
Na	mg/kg	1157.74549	1322.07662	1228.71884	1433.11411	1234.82571	1358.15534	874.622021	1262.90361
B	mg/kg	0	0.24258268	0.02462218	0.08156653	0.16999348	0.92706543	0.63936204	1.50878837
P	mg/kg	0.71917963	0.96565669	0.75335877	0.99235664	0.31814944	0.3552943	1.65975916	2.17259425
S	mg/kg	9.13242558	36.6056754	4.21120923	11.921107	258.109572	365.059629	91.6889469	383.220327

Sample A		Fresh (day 0)				Aged (day 84)			
Parameter	**Unit**	**Column test**		**Batch test**		**Column test**		**Batch test**	
L/S	**L/kg**	**2**	**10**	**2**	**10**	**2**	**10**	**2**	**10**
Se	mg/kg	0.00109105	0.00317603	0.00143192	0.00187075	0.00659785		0.04402622	0.19419707
Si	mg/kg	0	0	1.25107752	8.37677072	0	0	1.25833974	7.90745306
Ti	mg/kg	0.25830059	0.87751578	0.28653371	0.96252611	0.06113233	0.22641486		
Tl	mg/kg	2.803E-05	2.803E-05		0.00014391				
Fluoride	mg/kg								
Chloride	mg/kg	1358.71745	1723.71144	1389.36429	1752.14226	2197.7652	2369.12739	1670.52793	1869.23056
Nitrit	mg/kg	2.50176343	3.35994894	2.23474109	6.22279266			0.6673982	0.37454166
Bromide	mg/kg	2.55601751	2.56145533	2.23142774	2.2082475	37.5714037	37.8093001	12.0113282	8.13338132
Nitrate	mg/kg	0.10901881	0.10901881	0.21706673	0.31104441				
Sulfate	mg/kg	21.958757	79.608448	7.16051264	18.5226613	959.617137	1311.15485	413.873884	2027.33445
Phosphate	mg/kg					4.03305822	8.00501852	3.08811807	13.5977121
As	mg/kg	0.00048343	0.00133825	0.00017431	0.00062466	0.00184786	0.00613723		
Ba	mg/kg	13.3377687	37.6282985	20.9325277	43.7437299	0.07558724	0.78057299	0.64466305	1.79403981
Cd	mg/kg	0	0		0.000475	1.9666E-05	1.9666E-05	0.00034113	0.00112496
Cr	mg/kg	0.00959197	0.09706546	0.01040719	0.05417607	0.59385635	0.91714145	0.21181995	0.55131064
Cu	mg/kg	0.18091939	0.36330255	0.3391087	0.55899136	0.27991559	0.37513332	0.21511979	0.2473089
Hg	mg/kg	0.00041403	0.0023983	0.00014574		0.00183859	0.0081409	0.00066535	0.00273839
Mn	mg/kg	0	0.00317754		0.00132414	0.00112	0.00759934	2.5987E-05	
Mo	mg/kg	0.16512512	0.39459541	0.12459954	0.29091152	0.32129451	0.41353338	0.1799204	0.15671221
Ni	mg/kg	0.00257616	0.00257616	0.00110044	0.00433812	0.00152926	0.12415834	0.00283821	
Pb	mg/kg	0.46283388	1.43356125	1.17305275	1.54188298	0.00017225	0.00186682		
Sb	mg/kg	0.00137512	0.10963396	0.0142272	0.13220908	0.07759631	0.40932217	0.04303271	0.16419891
Sn	mg/kg	0.00128347	0.00516417	0.004067	0.01064607	0.00465767	0.04697978	0.00103495	0.00563394
Sr	mg/kg	7.18809208	13.1584368	9.09013184	12.2890545	0.78464285	3.20022275	0.96660329	2.97458844
V	mg/kg	0.00015093	0.00394017		0.00222336	0.01162817	0.04226116		
Zn	mg/kg	0.10111185	0.84380566	0.21348988	1.92276836	0	0.08625365	0.04003732	0.02564662
Co	mg/kg	0.00015738	0.00064661	9.4881E-05	0.000132	0.00078117	0.00224805		

Sample A		Fresh (day 0)				Aged (day 84)			
Parameter	Unit	Column test		Batch test		Column test		Batch test	
L/S	L/kg	2	10	2	10	2	10	2	10
Al	mg/kg	1.05881404	56.8265764	0.54935352	64.191654	88.9739667	306.882591	45.3207322	118.31534
Ca	mg/kg	1171.52829	3849.97703	1076.17633	2862.14656	192.654248	852.429716	218.228735	1064.27811
Fe	mg/kg	0	0	0.00036475	0.00086279	0	0		
K	mg/kg	416.250626	510.458626	439.902834	473.29697	358.248003	501.297259	298.432354	376.349013
Mg	mg/kg	0	0	0.04571632	0.04420201	0.10953631	0.10953631		
Na	mg/kg	1157.14638	1315.08339	1321.05312	1448.50709	1264.77238	1391.4947	888.956685	1273.92523
B	mg/kg	0	0.17040523	0.02145822	0.0495105	0.2307624	1.08138517	0.56626311	0.97548531
P	mg/kg	0.72637364	0.90307001	0.79112113	0.94911988	0.36405938	0.45398241	1.62359615	0.92772898
S	mg/kg	8.95988683	38.7106641	4.52598624	10.5463668	256.790882	361.469641	97.8445148	417.032229
Se	mg/kg	0.00109105	0.00378624	0.00076546	0.0033121	0.00818415	0.0128204	0.06158761	0.05444828
Si	mg/kg	0	0	1.24741144	8.42404929	0	0	1.16639974	3.09578033
Ti	mg/kg	0.27914381	0.85409743	0.29294182	0.92343859	0.05800426	0.23695412		
Tl	mg/kg	2.803E-05	2.803E-05		6.6232E-05				
Fluoride	mg/kg								
Chloride	mg/kg	1371.37257	1709.1953	1496.96992	1682.03876	2202.32528	2405.47034	1705.75816	1852.5241
Nitrit	mg/kg	2.44308203	3.41367638	2.45022134	6.1005772			0.40968696	0.27841673
Bromide	mg/kg	2.56145533	2.55601751	2.44256473	2.12010945	35.7548413	36.1408724	9.30000105	8.04982336
Nitrate	mg/kg	0.10901881	0.10901881	0.23280801	0.47180247				
Sulfate	mg/kg	21.2791885	80.9949205	7.73288996	18.3109124	917.31531	1258.54245	366.764431	1889.92572
Phosphate	mg/kg					4.14906498	7.02707382		13.8190042